WARWICK
THE UNIVERSITY OF WARWICK

Manuscript version: Author's Accepted Manuscript
The version presented in WRAP is the author's accepted manuscript and may differ from the published version or Version of Record.

Persistent WRAP URL:
http://wrap.warwick.ac.uk/144678

How to cite:
Please refer to published version for the most recent bibliographic citation information. If a published version is known of, the repository item page linked to above, will contain details on accessing it.

Copyright and reuse:
The Warwick Research Archive Portal (WRAP) makes this work by researchers of the University of Warwick available open access under the following conditions.

© 2020 Elsevier. Licensed under the Creative Commons Attribution-NonCommercial-NoDerivatives 4.0 International http://creativecommons.org/licenses/by-nc-nd/4.0/.

Publisher's statement:
Please refer to the repository item page, publisher's statement section, for further information.

For more information, please contact the WRAP Team at: wrap@warwick.ac.uk.

warwick.ac.uk/lib-publications

Journal Pre-proof

Orexin-A protects against cerebral ischemia-reperfusion injury by inhibiting excessive autophagy through OX1R-mediated MAPK/ERK/mTOR pathway

Dandan Xu[a,1], Tingting Kong[c,1], Shengnan Zhang[b], Baohua Cheng[b], Jing Chen[b,d]*, Chunmei Wang[b]*

[a] Cheeloo College of Medicine, Shandong University, Jinan, 250012, P.R. of China.

[b] Neurobiology Key Laboratory of Jining Medical University, Jining, 272067, P.R. of China.

[c] Caoxian People's Hospital, Heze, 274400, China

[d] Division of Biomedical Sciences, Warwick Medical School, University of Warwick, Coventry, CV4 7AL, UK.

[1] Equally contributed to this manuscript.

*Corresponding author Chunmei Wang: wangchunmei410@mail.jnmc.edu.cn

*Co-corresponding author Jing Chen: Jing.Chen@warwick.ac.uk

Journal Pre-proof

Abstract

Orexin A (OXA) is a neuroprotective peptide that exerts protective effects on multiple physiological and pathological processes. Activation of autophagy is linked to the occurrence of cerebral ischemia–reperfusion injury (CIRI); however, its function remains incompletely understood. In this study, OXA was sought to exert its neuroprotective role by regulating autophagy in oxygen and glucose deprivation and reoxygenation (OGD/R) model and middle cerebral artery occlusion (MCAO) model of rats, and to elucidate the underlying molecular mechanisms. Acridine orange (AO) staining was used to evaluate autophagic vacuoles. Cell viability was measured by CCK8. The levels of p-ERK$_{1/2}$, t-ERK$_{1/2}$, p-mTOR, LC3B, Beclin 1, and p62 were evaluated by western blotting. Apoptosis rate was detected by Hoechst 33342 staining and Terminal deoxynucleotidyltransferase–mediated dUTP nick-end labeling (TUNEL). OXA treatment alleviated neuronal apoptosis and significantly inhibited autophagy activity. Mechanistically, OXA exerted its neuroprotective effects in vivo and in vitro by suppressing over-activated autophagy by modulating OX1R-mediated MAPK/ERK/mTOR pathway. The results of this study elucidate the roles of autophagy in CIRI and the mechanisms underlying the neuroprotective action of OXA. Our findings could facilitate the development of novel therapeutics for ischemic stroke.

Keywords

Orexin-A (OXA); autophagy; cerebral ischemia–reperfusion injury (CIRI); oxygen–glucose deprivation/reoxygenation (OGD/R); neuroprotection.

Abbreviations: BP, biological process; CCK-8, Cell Counting Kit-8; CC, cellular component; DEGs, differentially expressed genes; DMEM, Dulbecco's modified Eagle's medium; FPKM, Fragments Per Kilobase of transcript sequence per Million base pairs sequenced; HSP, heat shock protein; IRI, ischemia-reperfusion injury;

Journal Pre-proof

lncRNA, long non-coding RNA; MF, molecular function; OGD/R, oxygen-glucose deprivation and reoxygenation

1. Introduction

Ischemic stroke, which is caused primarily by thrombosis and thromboembolism, is one of the most prominent fatal diseases worldwide (Sternberg and Schaller, 2020). The standard treatment is to restore blood perfusion to ischemic areas within a short time after the infarct. In some cases, however, restoration of blood flow after ischemia does not restore tissue function, but instead exacerbates tissue injury and dysfunction. This phenomenon, termed ischemia–reperfusion injury, can lead to serious tissue damage and organ dysfunction, and therefore represents an important clinical challenge (Marrone et al., 2018; Zhang et al., 2013).

Autophagy is the primary mechanism by which eukaryotic cells degrade excessive or abnormal protein organelles to maintain normal cellular function (Mizushima et al., 2008). Autophagy is a complex degradative pathway that plays key roles in cellular metabolism. In response to various stimuli, autophagy promotes lysosome phagocytic organelles and other cytoplasmic components with critical functions in the physiological and pathological processes of the cell (Xu and Zhang, 2011). This process is distinct from necrosis and apoptosis, and can be used as a form of cellular self-defense (Baehrecke, 2003).

Energy expenditure and hypoxia are the most powerful stimuli for autophagy, whereas low energy demand and oxygen repletion suppress autophagy. Moderate levels of autophagy catabolize the damaged, denatured, or aging proteins for recycling and re-utilization (Cuervo, 2004; Levine and Klionsky, 2004; Shintani and Klionsky, 2004). Traditionally, low-level autophagy is thought to be beneficial to cell survival (Scherz-Shouval et al., 2007). It is vital that the cells of the body maintain a basic, low level of autophagic activity. In the context of stroke, autophagy begins to be activated during the ischemic phase and continues to be active, or even hyperactive, during the reperfusion phase (Thapalia et al., 2014). Many studies have confirmed that

autophagy is involved in the pathophysiology of CIRI (Kotoda et al., 2018; Yu et al., 2019). One possible mechanism involves reductions in ATP levels after neuronal ischemia and hypoxia, leading to activation of autophagy through various pathways. Hence, although autophagy is certainly activated after CIRI, it remains unclear whether it is beneficial to damaged cells. The advantages and disadvantages of autophagy have been extensively studied. Chloroquine, an autophagy inhibitor, has a wide range of prospects for application as an antitumor drug; however, autophagy has a protective effect on acute renal injury, which may therefore be aggravated by chloroquine (Kimura et al., 2013). A large body of similar evidence supports the concept that autophagy is a double-edged sword (Chen-Scarabelli et al., 2014).

Orexin A (OXA) is a peptide secreted by hypothalamus that exerts its effects by binding to specific receptors, orexin receptor type 1 (OX1R) and type 2 (OX2R). OXA activates downstream signaling pathways primarily by binding OX1R (Shu et al., 2017), thereby influencing multiple physiological processes such as feeding behavior, sleep–wake rhythm, reward and addiction, and energy balance and pathological processes such as narcolepsy, depression, ischemic stroke, drug addiction and Alzheimer's disease (AD) (Davies et al., 2015; Feng et al., 2014). In particular, following CIRI, exogenous OXA mediates neuroprotection through HIF-1 (Yuan et al., 2011), and the protective effect of OXA on CIRI involves the reduction of oxidative stress (Bulbul et al., 2008). Preliminary work by our group confirmed that OXA protects neurons against I/R injury via the ERK signaling pathway *in vivo* [unpublished], and against H_2O_2 damage via the PI3K/MEK/ERK signaling pathway *in vitro* (Wang et al., 2018). In addition, we showed that OXA protects cells from damage induced by oxygen–glucose deprivation/reoxygenation (OGD/R) by inhibiting endoplasmic reticulum stress–mediated apoptosis (Kong et al., 2019).

However, the relationship between the neuroprotective effect of OXA and autophagy has not been examined in OGD/R or middle cerebral artery occlusion (MCAO) models. We hypothesized that OXA alleviates damage induced by OGD/R or MCAO by activating or inhibiting autophagy. Using an OGD/R model in SH-SY5Y cells and an MCAO model in Wistar rats, we investigated whether

regulation of autophagy contributes to the neuroprotective effect of OXA in cerebral ischemia–reperfusion injury (CIRI).

2. Materials and methods

2.1 Chemicals and reagents

Human OXA was obtained from Phoenix Pharmaceuticals (Belmont, CA, USA). Primary antibodies against p-ERK$_{1/2}$, t-ERK$_{1/2}$, p-mTOR, LC3B, Beclin 1, and p62 were purchased from Cell Signaling Technology (Danvers, MA, USA). Anti-β-actin antibody was obtained from BZSGB Technology (Beijing, China). U0126 (A selective inhibitor of MEK-1 and MEK-2), LY294002 (A specific inhibitor of phosphatidylinositol-3-kinase), PD98059 (Potent, selective and cell-permeable inhibitor of MAPK kinase, MAPK/ERK, or MEK), and SB334867 (A non-peptide selective antagonist of OX1R) were purchased from Sigma-Aldrich (St. Louis, MO, USA). Dulbecco's modified Eagle's medium (DMEM) and fetal bovine serum (FBS) were obtained from Gibco Life Technologies (Grand Island, NY, USA).

2.2 Cell culture and drug treatment

SH-SY5Y human neuroblastoma cells were obtained from the Cell Resource Center of the Chinese Academy of Sciences (Shanghai, China). SH-SY5Y cells were cultured in DMEM supplemented with 10% FBS, penicillin (100 U/ml), and streptomycin (100 U/mL) at 37°C in an atmosphere containing 95% air and 5% CO_2. When the cells in the dish are full, the cells are planted into the six-well plate and the twelve-well plate, each well is about 5×10^5 and 1×10^5 cells respectively, and then incubated for 24 h for the construction of the OGD/R model.

SH-SY5Y cells were treated with OXA (1×10^{-7}M) for 24 h at the onset of reperfusion. Cells were also treated with the SB334867 (1×10^{-6}M), U0126 (10μM) and LY294002 (10μM), 30 min before OXA treatment, respectivly.

2.3 OGD/R model

SH-SY5Y cells were cultured normally to 70–80% confluence and immediately placed in an atmosphere of 5% CO_2 and 90% N_2 for culture in glucose-free medium. After OGD for the indicated time, cells were returned to glucose-containing medium

and cultured under standard conditions (95% air and 5% CO_2).

We deprived SH-SY5Y cells of oxygen and glucose for 4 h (OGD 4h), and then re-exposed them to oxygen and glucose for 4 (R 4h), 12 (R 12h), and 24 h (R 24h). Then SH-SY5Y cells were divided into the untreated group (control), the treatment with OXA group (OXA), OGD 4 h/R 24 h group (OGD 4 h/R 24 h), OGD 4 h/R 24 h treatment with OXA group (OGD 4 h/R 24 h + OXA), OGD 4 h/R 24 h treatment with OXA and SB334867 (SB + OXA), the treatment with U0126 group (U0126), OGD 4 h/R 24 h treatment with U0126 group (OGD 4 h/R 24 h + U0126), OGD 4 h/R 24 h treatment with LY294002 group (LY).

2.4 Animals

Male wistar rats (weight, 230–250 g; 9-10 weeks) were purchased from Pengyue Experimental Animal Ltd. (Jinan, Shandong, China). 90 rats were housed at a constant temperature of 26 ± 2°C with humidity of 50–65%. All experimental procedures were approved by the Committee on Animal Care and Usage of Jining Medical University (approval No.2018-JU-001).

2.5 MCAO model

After weighing, rats were anesthetized intraperitoneally with 10% chloral hydrate (3 mL/kg), and the right common carotid artery (CCA) and external carotid artery (ECA) were isolated and ligated. An incision was made near the CCA ligation site, and a thread was gently pushed in until a slight resistance was felt. Plug insertion depth was 1.8–2.2 cm from the bifurcation of the CCA. After the thread plug was fixed, the separated muscle and skin were closed by stitching. After 2 h of ischemia, the thread plugs were removed to allow reperfusion. The sham operation group was the same as the model group except that the middle cerebral artery was not occluded.

The rats were randomly divided into the sham operation group (Sham), the MCAO model group and reperfusion 6 h (I/R 6h), I/R 6 h with intracerebroventricular (ICV) injection of OXA (OXA), I/R 6 h with ICV injection of OXA and SB334867 (SB+OXA), I/R 6 h with ICV injection of PD98059 (PD) and I/R 6 h with ICV injection of normal saline (NS).

2.6 Intracerebroventricular injection

Journal Pre-proof

Intervention drugs were injected into lateral ventricle; OXA (30μg/kg) and PD98059 (10μM) were administered during reperfusion after ischemia for 2 h, and SB334867 (2.4mM) was administered 30 min before OXA. Anesthetized rats in the prone position were fixed on the brain stereotaxic apparatus, the anterior fontanelle was exposed, and marks were made 0.8 mm behind the anterior fontanelle and 1.6 mm laterally. A micro-electric cranial drill was used to drill holes. The needle of the microsyringe slowly penetrated 3.8 mm below the skull for drug injection (2 μl/min).

2.7 Cell Counting Kit-8 (CCK-8) assay

After cells cultured in 96-well plates were treated, cell proliferation and cell viability were measured using the Cell Counting Kit-8 (CCK-8) assay (KeyGEN BioTECH, Nanjing, China). Each well was incubated with 10 μL of CCK-8 reagent for 2 h, and optical density (OD) at 450 nm was measured on a microplate reader (Bio-Rad, Hercules, CA, USA) to determine cell viability.

2.8 Hoechst 33342 staining

Apoptosis was evaluated by Hoechst 33342 staining. Briefly, the cells of each group were treated on 12-well culture plates, washed with PBS, and then incubated with 1 ml of cell staining buffer containing 5 μl of Hoechst staining solution and 5 μl of PI staining solution. After mixing, the cells were stained at 4 °C for 20 min, washed twice with PBS, and visualized under the microscope. Image processing and analysis were performed using the ImageJ2x software.

2.9 Acridine orange (AO) staining

AO staining labels acidic vesicle organelle structures, such as autophagosomes. Cells were cultured in 24-well plates. After treatment, they were washed with PBS, and each well was stained with 2 ml AO (5 mg/ml, Sigma-Aldrich) for 25 min at 37 °C. Images were obtained on an Olympus fluorescence microscope, and image processing and analysis were carried out with the ImageJ2x software.

2.10 Preparation of frozen slices

After reperfusion for 6 h, rats were fixed on the operating table and perfused from the left ventricle with PBS and 4% paraformaldehyde (PFA) until stiff. Brain samples were fixed with 4% PFA for 24 h, and dehydrated with 30% sucrose solution until

they sunk, which took about 2–3 d. A frozen microtome (Thermo Fisher Scientific, Waldorf, Germany) was used to make continuous sections in coronal position (30 μm) and stored in antifreeze buffer at -20 °C.

2.11 Terminal deoxynucleotidyltransferase–mediated dUTP nick-end labeling (TUNEL)

Frozen sections were taken out and stabilized at room temperature for 15 min. The slices were then fixed with freshly prepared 4% PFA for 30 min and permeabilized with Proteinase K (20 μg/ml) for 5 min. After each sample was equilibrated with 100 μl of equilibration buffer, 50 μl rTdT Reaction Buffer was added. Samples were then incubated with 2×SSC for 15 min, and DAPI (100 ng/ml) was used to dye the nuclei for 30 min. Images were visualized and collected by inverted fluorescence microscopy (IX 71; Olympus, Tokyo, Japan).

2.12 Western blotting assay

Adherent cell samples were lysed using RIPA lysis buffer, and the extracted proteins were separated by sodium dodecyl sulfate–polyacrylamide gel electrophoresis (SDS-PAGE). Then the protein is transferred to the PVDF membrane by wet transfer. After transfer, membranes were washed with Tris-buffered saline + Tween (TBST) for 10 min, and then blocked with 5% skim milk at room temperature for 1 h. After washing with TBST, the membrane was incubated at 4°C overnight with the appropriately diluted primary antibody: rabbit anti-p-ERK$_{1/2}$, mouse anti-t-ERK$_{1/2}$, rabbit anti-p-mTOR, rabbit anti-LC3B, rabbit anti-Beclin 1, mouse anti-p62 (1:1000; Cell Signaling Technology), and mouse anti-β-actin (1:1,000; Zhongshan Golden Bridge Biotechnology). The next day, the membrane was incubated with the corresponding horseradish peroxidase–labeled secondary antibody (1:5000; Zhongshan Golden Bridge Biotechnology) for 1 h at room temperature. Finally, the bands were revealed using an ECL kit (liankebio, Hangzhou, China). Image processing and analysis were carried out with the ImageJ2x software.

2.13 Statistical analysis

Results are expressed as means ± standard deviation. One-way ANOVA followed by Tukey test was performed using GraphPad Prism (GraphPad Software, Inc., La Jolla,

CA, USA). Multiple comparison between groups was performed using the S-N-K method. $p<0.05$ was considered significant. All data shown are representative of at least three independent experiments.

3. Results

3.1 OGD/R triggers activation of autophagy

To observe the dynamic changes of autophagy in an *in vitro* model of ischemic injury, we performed AO staining to evaluate autophagic vacuoles. As shown in Figure 1A, the proportion of cells with red-stained autophagic vacuoles was 7.59% in control, 11.40% at OGD 4h, 16.66% at R 4h, 16.67% at R 12h, and 21.18% at R 24h. Relative to the control, red-stained autophagic vacuoles were significantly more abundant after OGD/R injury ($p<0.05$), and their abundance gradually increased with reperfusion time ($p<0.01$), indicating that both oxygen–glucose deprivation and reperfusion injury significantly activate autophagy activity.

To further verify the activation of autophagy by OGD/R injury, we analyzed the expression of autophagic markers by Western blotting. As shown in Figure 1B, the levels of LC3B-I and LC3B-II in the control group were very low. LC3B-II was clearly induced at various reperfusion times; but LC3B-I was meaningfully induced only at R 24h, causing the LC3B-II/LC3B-I ratio to significantly increase ($p<0.05$). Moreover, with prolonged reperfusion, the level of Beclin 1 gradually increased ($p<0.05$), especially at R 24h. By contrast, the level of p62 significantly reduced ($p<0.05$) after OGD/R injury. Together, these results confirm that OGD/R triggers autophagic activation.

3.2 OXA combined with OX1R protects against OGD/R injury

Our previous studies confirmed the protective effect of OXA following OGD/R (Kong et al., 2019). In this study, to further clarify the protective mechanism of OXA, we treated cells with SB334867(SB), an OX1R antagonist.

To verify that OXA protects against OGD/R injury when combined with OX1R, we used the CCK-8 assay to measure cell viability. The trend in the change of cell

viability was basically the same in the OGD 4 h/R24 h models. Compared with untreated cells (control group), the viability of SH-SY5Y cells were decreased by about 39.28% after OGD 4 h/R 24 h (p<0.001) (Figure 2A). After OXA treatment, cell viability increased by about 21.34 % (p<0.01) relative to the OGD/R-treated groups. When OGD/R-treated cells were subsequently treated with the combination of SB and OXA, cell viability was decreased by about 17.25 % in OGD 4h/R 24h model (p<0.01), relative to OXA alone. The results confirmed that OXA could alleviate the decline in cell viability induced by OGD/R. However, after co-treatment with SB, the protective effect of OXA was weakened, indicating that OXA increases cell viability in combination with OX1R in the OGD/R *in vitro* model.

To further confirm that OXA in combination with OX1R protects against OGD/R injury, we performed Hoechst 33442 staining to detect apoptosis. The results were consistent with our viability measurements, and the changes were essentially the same between the two groups. The apoptotic frequencies were 28.70% in the OGD 4h/R 24h models (p<0.01). OXA treatment significantly decreased the apoptotic frequencies to 13.15% (p<0.05). Similarly, in the co-intervention groups of SB and OXA, the apoptotic frequencies increased by 13.59% relative to the OXA group alone (p<0.05) (Figure 2B). These results confirm that inhibition of OGD/R-induced apoptosis induced by OXA is dependent on the combination with OX1R.

3.3 OXA inhibits activation of autophagy

After confirming that OGD/R activates autophagy and OXA has a protective effect against the OGD/R injury, we speculated that OXA plays its protective role by affecting autophagic activity. As shown in Figure 3A, after OGD 4h/R 24h injury, the LC3B-II/LC3B-I ratio and level of Beclin 1 were significantly higher than in the control (p<0.05), whereas both parameters significantly decreased in the OXA-treated group (p<0.05). Thus, we inferred that OXA protects against OGD/R injury by preventing the overactivation of autophagy.

Next, we used SB to investigate whether the effect of OXA on autophagy is the result of binding to OX1R. As shown in Figure 3B, compare to the OXA-treated group, the LC3B-II/LC3B-I ratio and level of Beclin 1 in the co-intervention group

(OXA + SB) were significantly elevated after OGD 4h/R 24h (p<0.05). Thus, SB treatment blocked the effect of OXA on autophagy.

AO staining also supported our results. Compared with the control group, the number of autophagic vacuoles was significantly higher by 18.08% in the OGD 4h/R 24h models (p<0.01). The number of autophagic vacuoles was decreased by about 12.44% in the OXA-treated group relative to the OGD 4h/R 24h group (p<0.05), but increased by about 16.09 % in the OXA + SB co-intervention group relative to the OXA-treated group (p<0.01) (Figure 3C).

Together, these experiments demonstrated that OXA exerts a protective effect by inhibiting overactivation of autophagy.

3.4 U0126 inhibits autophagy by inhibiting ERK phosphorylation

We know that mTOR is a key regulator of the upstream pathway regulating autophagy (Laplante and Sabatini, 2012), and that the ERK signaling pathway also can regulate autophagy (Kim et al., 2014). In this study, we found that the level of p-mTOR protein decreased over time and with aggravation of OGD/R injury, in contrast to the levels of autophagy-related proteins and p-ERK. As shown in Figure 4A, relative to the control group, the level of p-$ERK_{1/2}$ increased significantly after OGD/R treatment (p<0.05), whereas the level of p-mTOR significantly decreased (p<0.05).

We used U0126, an ERK-specific inhibitor, to confirm that ERK is a regulator of the upstream pathway that regulates autophagic activation during OGD/R injury. In comparison with cells treated with OGD/R alone, treatment with U0126 significantly decreased the level of p-$ERK_{1/2}$ (p<0.01) and increased the level of p-mTOR (p<0.05) (Figure 4B). Similarly, U0126 significantly decreased the LC3B-II/LC3B-I ratio and level of Beclin 1 (p<0.05 and p<0.01), whereas LY294002 did not meaningfully change either value (Figure 4C).

Next, we performed AO staining to determine the abundance of autophagic vacuoles. Relative to cells treated with OGD/R alone, cells treated with U0126 had significantly fewer red-stained autophagic vacuoles (5.48%, p<0.05) (Figure 4D). These results indicate that autophagy is regulated following OGD/R injury by

upstream ERK signaling

3.5 OXA protects against CIRI *in vivo*

CIRI triggers autophagy activation. We then sought to validate the results of our *in vitro* experiments in intact animals. Due to limitations on modeling and drug intervention methods, we only conducted the corresponding intervention in a rat ischemia–reperfusion model. To verify that autophagy was induced by CIRI, we monitored the levels of autophagy markers by Western blotting. As shown in Figure 5A, as reperfusion time after CIRI increased, the LC3B-II/LC3B-I ratio and level of Beclin 1 were significantly elevated relative to the Sham group ($p<0.05$ and $p<0.01$), whereas the level of p62 was significantly reduced ($p<0.05$ and $p<0.01$). Therefore, CIRI indeed activates autophagy.

OXA intervention inhibits activation of autophagy after CIRI. We speculated that in rats, as in our cell experiments, OXA plays its role by affecting autophagic activity. As shown in Figure 5B, relative to the Sham group, the LC3B-II/LC3B-I ratio and level of Beclin 1 were significantly elevated after CIRI ($p<0.05$ and $p<0.01$), but significantly reduced in the OXA-treated group ($p<0.05$ and $p<0.01$). At this point, we inferred that OXA protects against CIRI by preventing overactivation of autophagy. Furthermore, the LC3B-II/LC3B-I ratio and level of Beclin 1 after CIRI were significantly higher in the OXA + SB co-treatment group ($p<0.05$). These results demonstrate that SB intervention blocks the effect of OXA on autophagy.

OXA in combination with OX1R inhibited CIRI-induced apoptosis. We next sought to determine whether OXA could inhibit CIRI-induced apoptosis, and if so, how. A TUNEL assay revealed that the apoptotic frequency was 32.0% in the I/R 6h model ($p<0.01$), whereas OXA treatment decreased this value to 22.9% ($p<0.05$). Similarly, in the co-intervention group (SB + OXA), the apoptotic frequency increased by 19.0% relative to the OXA-alone group ($p<0.05$) (Figure. 5C). These results confirm that inhibition of CIRI-induced apoptosis by OXA depends on OX1R.

3.6 PD98059 inhibits autophagy by inhibiting ERK phosphorylation

Consistent with the results of our cell experiments, treatment with PD98059

Journal Pre-proof

significantly decreased the LC3B-II/LC3B-I ratio and level of Beclin 1 relative to the I/R 6h group, ($p<0.05$) (Figure 6). Treatment with normal saline (NS) did not result in meaningful changes, indicating that autophagy in CIRI could be regulated by ERK1/2 signaling pathway.

4. Discussion

OXA is a neuropeptide expressed mainly in the lateral hypothalamus. Initial research on OXA focused on its role in regulating the body's food intake and energy balance. However, in this study, from the perspective of cell proliferation and apoptosis, OXA exerted a neuroprotective effect by inhibiting autophagy in model of OGD/R. To the best of our knowledge, we first confirmed that normal cultures exhibited the expected low level of autophagy, and then verified that autophagy was activated after OGD/R. However, OXA decreased the levels of autophagy-related proteins and the number of autophagic vacuoles.

To validate our *in vitro* results, we also performed *in vivo* experiments. We found that if we injected OXA into the lateral ventricle, the mortality rate was very high, potentially because the rats were in a supine position, which allowed the cerebrospinal fluid to easily flow out after the skull was drilled. Therefore, we injected the OXA at the same time as reperfusion, and then performed related tests. OXA treatment decreased the levels of autophagy-specific proteins. In combination with the results of our cell experiments, our *in vivo* model demonstrated that with aggravation of injury, excessive activation of autophagy results in cell injury or even death.

These findings are consistent with the pathological mechanisms of many diseases previously reported that the main function of low-level autophagy is to eliminate damaged proteins from cells, whereas excessive activation of autophagy causes the degradation of large quantities of cytoplasmic proteins and self-digestion of organelles, resulting in loss of cellular function and even cell death. For example, autophagy in intestinal mucosa is significantly upregulated after intestinal I/R, and inhibition of autophagy can alleviate the resultant damage (Li et al., 2019). Gastrodin inhibits autophagy in neonatal rat cardiomyocytes by activating mTOR signaling and protects cardiomyocytes from hypoxia/reoxygenation injury (Li et al., 2018b). In

addition, 002C-3, a newly synthesized derivative of magnolol, exerts neuroprotective effects following CIRI in rats by inhibiting hyperactive autophagy (Li et al., 2015).

Many pathophysiological processes are involved in CIRI, but due to the complexity of the underlying mechanism, the role of autophagy in it cannot be simply concluded as the function of protection or the effect of injury. Studies of the function of OXA have confirmed that in pancreatic cancer, OXA treatment activates the Akt/mTOR signaling pathway, promoting cell proliferation by inhibiting apoptosis mediated by Bcl-2, caspase-9, and c-myc (Suo et al., 2018). In our study of CIRI, we found that OXA plays a neuroprotective role by regulating autophagy through inhibiting it after oxygen and glucose deprivation and reoxygenation, ultimately decreasing apoptosis and promoting cell viability or cell proliferation. Autophagy plays an important role in the pathogenesis of ischemic heart disease. Its activation in the ischemic phase is beneficial to damage repair, while its activation in the reperfusion phase is harmful. Reperfusion injury is thought to be a result of dysregulation of autophagy (Baehrecke, 2003). We hypothesized that autophagy plays distinct roles at different stages of CIRI. Based on the experiments described in this manuscript, we can draw a preliminary conclusion: CIRI leads to activation of autophagy. Initially, autophagy serves to clear abnormal cell structures such as damaged organelles and also provide energy, allowing cells to stabilize their shape and structure, maintain their normal functions, and improve their chances of survival after CIRI. Its role in cell survival is consistent with our observations of cells exposed to OGD 4h. The level of autophagy increased significantly at the 24 h after OGD/R, which was also the case in the MCAO model in rats. Excessive activation of autophagy will cause cell damage or even death, and inhibition of autophagy will be beneficial to the repair of CIRI.

Autophagy is precisely regulated by multiple signaling pathways, including PI3K/AKT/mTOR (Li et al., 2018a; Vergadi et al., 2017) and Ras/Raf/MEK/$ERK_{1/2}$ (Choi et al., 2015; Kyriakakis et al., 2017; Yiu et al., 2018). The mechanism by which the PI3K/AKT/mTOR signaling pathway regulates autophagy has been extensively studied. Hence, we also examined this pathway in the OGD/R model used in our experiments; however, we detected no changes in the expression of AKT, suggesting

that autophagy may be induced by a different pathway in our experimental model. In our study, changes in the expression of $ERK_{1/2}$ were predominant. In recent years, several studies have shown that both activation and inhibition of the Ras/Raf/MEK/$ERK_{1/2}$ signaling pathway can induce autophagy, but the specific mechanism remains unknown. In particular, very little information is available regarding the signaling pathways leading to autophagy in CIRI. We treated OGD/R-injured cells with the $ERK_{1/2}$-specific inhibitor U0126 and the PI3K inhibitor LY294002, and treated rats with PD98059. We found that U0126 and PD98059 decreased the expression of autophagy-related proteins in ischemia–reperfusion injury. Intervention with LY294002 did not cause statistically significant changes, and the results of AO staining were consistent with the protein levels (Figure 4). Given that autophagy in CIRI is mainly regulated by $ERK_{1/2}$, we will need to use other specific blockers to determine whether it is equally effective in blocking other key molecules in the Ras/Raf/MEK/$ERK_{1/2}$ signaling pathway.

It is clear that autophagy is upregulated after CIRI, but its role in disease development remains controversial. Moreover, the specific role of autophagy in CIRI, as well as the underlying mechanism, remain unclear. Therefore, other key targets in the autophagy pathway and the specific molecular mechanism of autophagy causing CIRI need to be further explored, which will help to develop drugs for the treatment of stroke. In addition, it is worth mentioning that the ICV flow velocity of the OXA in this experiment was 2μl/min. Although we did not find significant adverse reactions in the rats, the slowing down of the drug flow rate may be more beneficial to the survival of the rats and prolong the survival time after surgery.

In summary, autophagy, a fundamental biological phenomenon, is intimately involved in the physiological and pathological process of CIRI. In the case of mild ischemia and hypoxia, autophagy is moderately activated and plays a neuroprotective role, whereas in the case of reperfusion injury, autophagy is overactivated. Autophagy is regulated by $ERK_{1/2}$, and the neuroprotective effect of OXA in combination of OX1R is mediated by its effects on autophagy, which ultimately decrease the rate of apoptosis and increase cell viability or cell proliferation (Figure 7). The results of this

study clarify the role of autophagy in CIRI and the mechanism underlying the neuroprotective action of OXA. These findings should provide novel directions for therapeutic treatment of ischemic stroke.

Journal Pre-proof

ACKNOWLEDGEMENTS

This work was supported by Research Fund for Academician Lin He New Medicine (JYHL2019ZD02).

AUTHOR CONTRIBUTIONS

Chunmei Wang conceived and designed the experiments; Dandan Xu and Tingting Kong conducted the experiments and wrote the manuscript; Shengnan Zhang performed the data analysis; Jing Chen and Baohua Cheng revised the manuscript.

CONFILICT OF INTEREST

The authors confirm that there are no conflicts of interest.

Journal Pre-proof

References

Baehrecke, E.H., 2003. Autophagic programmed cell death in Drosophila. Cell Death Differ. 10**,** 940-5.

Bulbul, M., et al., 2008. Effect of orexin-a on ischemia-reperfusion-induced gastric damage in rats. J Gastroenterol. 43**,** 202-7.

Bursch, W., 2001. The autophagosomal-lysosomal compartment in programmed cell death. Cell Death Differ. 8**,** 569-81.

Chen-Scarabelli, C., et al., 2014. The role and modulation of autophagy in experimental models of myocardial ischemia-reperfusion injury. J Geriatr Cardiol. 11**,** 338-48.

Choi, J., et al., 2015. Dienogest enhances autophagy induction in endometriotic cells by impairing activation of AKT, ERK1/2, and mTOR. Fertil Steril. 104**,** 655-64 e1.

Cuervo, A.M., 2004. Autophagy: in sickness and in health. Trends Cell Biol. 14**,** 70-7.

Davies, J., et al., 2015. Orexin receptors exert a neuroprotective effect in Alzheimer's disease (AD) via heterodimerization with GPR103. Sci Rep. 5**,** 12584.

Feng, Y., et al., 2014. Neuroprotection by Orexin-A via HIF-1alpha induction in a cellular model of Parkinson's disease. Neurosci Lett. 579**,** 35-40.

Grafe, L.A., Bhatnagar, S., 2018. Orexins and stress. Front Neuroendocrinol. 51**,** 132-145.

Hu, Y., et al., 2014. High basal level of autophagy in high-altitude residents attenuates myocardial ischemia-reperfusion injury. J Thorac Cardiovasc Surg. 148**,** 1674-80.

Kim, J.H., et al., 2014. Raf/MEK/ERK can regulate cellular levels of LC3B and SQSTM1/p62 at expression levels. Exp Cell Res. 327**,** 340-52.

Kimura, T., et al., 2013. Chloroquine in cancer therapy: a double-edged sword of autophagy. Cancer Res. 73**,** 3-7.

Kong, T., et al., 2019. Orexin-A protects against oxygen-glucose deprivation/reoxygenation-induced cell damage by inhibiting endoplasmic reticulum stress-mediated apoptosis via the Gi and PI3K signaling pathways. Cell Signal. 62**,** 109348.

Kotoda, M., et al., 2018. Role of Myeloid Lineage Cell Autophagy in Ischemic Brain Injury. Stroke. 49**,** 1488-1495.

Kyriakakis, E., et al., 2017. T-cadherin promotes autophagy and survival in vascular smooth muscle cells through MEK1/2/Erk1/2 axis activation. Cell Signal. 35**,** 163-175.

Laplante, M., Sabatini, D.M., 2012. mTOR signaling in growth control and disease. Cell. 149**,** 274-93.

Levine, B., Klionsky, D.J., 2004. Development by self-digestion: molecular mechanisms and biological functions of autophagy. Dev Cell. 6**,** 463-77.

Li, B., et al., 2019. Inhibition of Autophagy Attenuated Intestinal Injury After Intestinal I/R via mTOR Signaling. J Surg Res. 243**,** 363-370.

Li, H., et al., 2015. Magnolol derivative 002C-3 protects brain against

ischemia-reperfusion injury via inhibiting apoptosis and autophagy. Neurosci Lett. 588**,** 178-83.

Li, W.D., et al., 2018a. LncRNA WTAPP1 Promotes Migration and Angiogenesis of Endothelial Progenitor Cells via MMP1 Through MicroRNA 3120 and Akt/PI3K/Autophagy Pathways. Stem Cells. 36**,** 1863-1874.

Li, X., et al., 2018b. Gastrodin protects myocardial cells against hypoxia/reoxygenation injury in neonatal rats by inhibiting cell autophagy through the activation of mTOR signals in PI3K-Akt pathway. J Pharm Pharmacol. 70**,** 259-267.

Marrone, L., et al., 2018. Isogenic FUS-eGFP iPSC Reporter Lines Enable Quantification of FUS Stress Granule Pathology that Is Rescued by Drugs Inducing Autophagy. Stem Cell Reports. 10**,** 375-389.

Mizushima, N., et al., 2008. Autophagy fights disease through cellular self-digestion. Nature. 451**,** 1069-75.

Scherz-Shouval, R., et al., 2007. Reactive oxygen species are essential for autophagy and specifically regulate the activity of Atg4. EMBO J. 26**,** 1749-60.

Shintani, T., Klionsky, D.J., 2004. Autophagy in health and disease: a double-edged sword. Science. 306**,** 990-5.

Shu, Q., et al., 2017. Orexin-A promotes Glu uptake by OX1R/PKCalpha/ERK1/2/GLT-1 pathway in astrocytes and protects co-cultured astrocytes and neurons against apoptosis in anoxia/hypoglycemic injury in vitro. Mol Cell Biochem. 425**,** 103-112.

Sternberg, Z., Schaller, B., 2020. Central Noradrenergic Agonists in the Treatment of Ischemic Stroke-an Overview. Transl Stroke Res. 11**,** 165-184.

Suo, L., Chang, X., Zhao, Y., 2018. The Orexin-A-Regulated Akt/mTOR Pathway Promotes Cell Proliferation Through Inhibiting Apoptosis in Pancreatic Cancer Cells. Front Endocrinol (Lausanne). 9**,** 647.

Thapalia, B.A., Zhou, Z., Lin, X., 2014. Autophagy, a process within reperfusion injury: an update. Int J Clin Exp Pathol. 7**,** 8322-41.

Vergadi, E., et al., 2017. Akt Signaling Pathway in Macrophage Activation and M1/M2 Polarization. J Immunol. 198**,** 1006-1014.

Wang, C.M., et al., 2018. Orexin-A protects SH-SY5Y cells against H2O2-induced oxidative damage via the PI3K/MEK1/2/ERK1/2 signaling pathway. Int J Immunopathol Pharmacol. 32**,** 2058738418785739.

Xu, M., Zhang, H.L., 2011. Death and survival of neuronal and astrocytic cells in ischemic brain injury: a role of autophagy. Acta Pharmacol Sin. 32**,** 1089-99.

Yiu, S.P.T., et al., 2018. Intracellular Iron Chelation by a Novel Compound, C7, Reactivates Epstein(-)Barr Virus (EBV) Lytic Cycle via the ERK-Autophagy Axis in EBV-Positive Epithelial Cancers. Cancers (Basel). 10.

Yu, S., et al., 2019. KCNQ1OT1 promotes autophagy by regulating miR-200a/FOXO3/ATG7 pathway in cerebral ischemic stroke. Aging Cell. 18**,** e12940.

Yuan, L.B., et al., 2011. Neuroprotective effect of orexin-A is mediated by an increase of hypoxia-inducible factor-1 activity in rat. Anesthesiology. 114**,** 340-54.

Zhang, X., et al., 2013. Cerebral ischemia-reperfusion-induced autophagy protects against neuronal injury by mitochondrial clearance. Autophagy. 9**,** 1321-33.

Journal Pre-proof

Figure Legends

Fig. 1 Autophagic vacuoles and Autophagy marker proteins in the SH-SY5Y OGD/R model are significantly increased

A. Autophagic vacuoles were assessed by AO staining under a fluorescence microscope (Bar=50μm). Red-stained autophagic vacuoles were significantly more abundant after OGD/R injury. B. Autophagy marker proteins were detected by Western blotting. The LC3B-II/LC3B-I ratio and level of Beclin 1 were significantly elevated after OGD/R treatment, whereas the level of p62 was reduced. *p<0.05 and **p<0.01 vs. the control group. Data are represented as means ± SEM (n=3). OGD: oxygen-glucose deprivation; R: reperfusion; AO: acridine orange; LC3B: microtubule-associated protein 1 light chain 3.

Fig. 2 Effect of OXA and SB334867 on cell viability and apoptosis in the SH-SY5Y OGD/R model

A. Cells were subjected to OGD/R and treated with or without OXA and SB; viability was monitored by CCK-8 assay. B. Cells were subjected to OGD 4h/R 24h and treated with or without OXA and SB; apoptosis was detected by Hoechst 33442 staining. **p<0.01, and ***p<0.001vs. the control group; $^{\#}p$<0.05 and $^{\#\#}p$<0.01vs. the OGD 4 h/R 24 h group; $^{\&}p$<0.05 and $^{\&\&}p$<0.01 vs. the OGD 4 h/R 24 h + OXA group. Data are represented as means ± SEM (n=3). OXA: Orexin-A; OGD: oxygen-glucose deprivation; R: reperfusion; SB: SB334867.

Journal Pre-proof

Fig. 3 Levels of autophagy marker proteins and Autophagic vacuoles following OXA and SB treatment

A. Cells were subjected to OGD 4h/R 24h and treated with or without OXA, and the levels of autophagy marker proteins were measured by Western blot.. The LC3B-II/LC3B-I ratio and level of Beclin 1 were significantly elevated after OGD/R treatment, but subsequently decreased after treatment with OXA. *p<0.05 vs. the control group; $^{\#}p$<0.05 vs. OGD 4h/R 24 h group. B. Cells were subjected to OGD 4h/R 24h and treated with or without SB, and the levels of autophagy marker proteins were measured by Western blot. The LC3B-II/LC3B-I ratio and level of Beclin 1 were significantly elevated after SB treatment. *p<0.05 vs. OGD 4h/R 24h + OXA group. C. Cells were subjected to OGD 4h/R 24h and treated with or without OXA and/or SB. The number of red-stained autophagic vacuoles is shown. *p<0.05 vs. OGD 4h/R 24h group; $^{\#\#}p$<0.01 vs. OGD 4h/R 24h + OXA group. (Bar=50μm). Data are represented as means ± SEM (n=3). OXA: Orexin-A; OGD: oxygen-glucose deprivation; R: reperfusion; SB: SB334867; LC3B: microtubule-associated protein 1 light chain 3.

Fig. 4 Effect of U0126 and LY294002 on autophagy marker proteins and Autophagic vacuoles in the SH-SY5Y OGD/R model

A. p-ERK$_{1/2}$ and p-mTOR were detected by Western blotting. The level of p-ERK$_{1/2}$ was significantly elevated after OGD/R treatment, whereas the level of p-mTOR was reduced. *p<0.05

vs. the control group. B: After addition of kinase inhibitor U0126, levels of p-$ERK_{1/2}$ and p-mTOR were detected by Western blot. In OGD/R-treated cells exposed to kinase inhibitors, treatment with U0126 significantly decreased the level of p-$ERK_{1/2}$ and increased the level of p-mTOR. **p*<0.05 and ***p*<0.01 vs. OGD 4h/R 24h group. C: After addition of U0126 and LY294002, levels of autophagy marker proteins were detected by Western blot. In OGD/R-treated cells exposed to kinase inhibitors, treatment with U0126 significantly decreased the LC3B-II/LC3B-I ratio and the level of Beclin 1, whereas treatment with LY294002 did not cause a significant change. **p*<0.05 and ***p*<0.01 vs OGD 4h/R 24h group. D: Number of autophagic vacuoles after treatment with kinase inhibitors U0126 and LY294002 (Bar = 50μm). In OGD/R-treated cells exposed to kinase inhibitors, treatment with U0126 significantly decreased the number of red-stained autophagic vacuoles, whereas treatment with LY294002 did not cause a significant change. **p*<0.05 vs. OGD 4h/R 24h group. Data are represented as means ± SEM (n=3). OGD: oxygen-glucose deprivation; R: reperfusion; LC3B: microtubule-associated protein 1 light chain 3; mTOR: mammalian target of rapamycin; LY: LY294002.

Fig.5 Effect of OXA and SB334867 on autophagy marker proteins and apoptosis *in vivo.*

A. Expression of autophagy marker proteins was detected in animal models by Western blotting. The LC3B-II/LC3B-I ratio and level of Beclin 1 were significantly elevated after I/R treatment, whereas the level of p62 was reduced. **p*<0.05 and ***p*<0.01 vs Sham group. B. Expression of autophagy marker proteins was determined by Western blotting in animal models: Levels of autophagy marker proteins in I/R 6h animals exposed to OXA and treated or not treated with SB.

The LC3B-II/LC3B-I ratio and level of Beclin 1 were significantly elevated after SB treatment. *p<0.05 and **p<0.01 vs. Sham group; $^{\#}p$<0.05 and $^{\#\#}p$<0.01vs. I/R 6h group; $^{\&}p$<0.05 vs. OXA intervention group. C. Apoptosis were determined by TUNEL staining in animal models. The TUNEL assay revealed that the apoptotic frequency was elevated in the I/R 6h model, and that OXA treatment significantly decreased IRI-induced apoptosis. Conversely, in the co-treatment group (SB + OXA), the apoptotic frequency was elevated. **p<0.01 vs Sham group; $^{\#}p$<0.05 vs. I/R 6h group; $^{\&}p$<0.05 vs. OXA group. Data are represented as means ± SEM (n=3). OXA: Orexin-A; SB: SB334867; I/R: ischemia-reperfusion; LC3B: microtubule-associated protein 1 light chain 3; DAPI: 4′,6-Diamidino-2-phenylindole; TUNEL: Terminal deoxynucleotidyltransferase–mediated dUTP nick-end labeling.

Fig. 6 PD98059 treatment inhibits autophagy *in vivo*.

After addition of kinase inhibitor PD98059, autophagy markers were detected by Western blotting. In in I/R 6h animals exposed to kinase inhibitors, treatment with PD98059 significantly decreased the LC3B-II/ LC3B-I ratio and level of Beclin 1. *p<0.05 vs. I/R 6h group. Data are represented as means ± SEM (n=3). I/R: ischemia-reperfusion; PD: PD98059; NS: Normal saline; LC3B: microtubule-associated protein 1 light chain 3.

Fig. 7 Schematic diagram of the mechanism of OXA inhibiting autophagy.

Autophagy during OGD/R and CIRI are regulated by the MAPK/$ERK_{1/2}$ pathway. Phosphorylated

Journal Pre-proof

mTOR inhibits autophagy. $ERK_{1/2}$, which acts upstream of mTOR, directly regulates autophagy or indirectly regulates autophagy through negative regulation of mTOR. LC3-II is a specific component of the autophagosome membrane, and Beclin 1 is essential for the formation of autophagic vacuoles. The autophagosome and lysosome combine to form the autophagolysosome, where contents are degraded. Treatment with U0126 inhibits autophagy. OXA reduces the phosphorylation level of $ERK_{1/2}$ by combining with OX1R in CIRI (unpublished). OXA binds to OX1R partially down-regulate autophagy to exert its neuroprotective effects via regulating MAPK/ $ERK_{1/2}$/mTOR pathway during OGD/R and CIRI. OGD/R: oxygen-glucose deprivation/reperfusion; CIRI: cerebral ischemia–reperfusion injury: OX1R: orexin receptor type 1.

Journal Pre-proof

Chunmei Wang conceived and designed the experiments;

Dandan Xu and Tingting Kong conducted the experiments and wrote the manuscript;

Shengnan Zhang performed the data analysis;

Jing Chen and Baohua Cheng revised the manuscript.

Journal Pre-proof

1. Orexin-A (OXA) is neuroprotective against cerebral ischemia–reperfusion injury (CIRI).

2. Orexin-A (OXA) decreased the autophagic biomarkers of the cortex in MCAO/R rat model and in SH-SY5Y human neuroblastoma cells subjected to OGD/R.

3. Orexin-A protects against cerebral ischemia-reperfusion injury by inhibiting excessive autophagy through OX1R-mediated MAPK/ERK/mTOR signaling pathway.

Journal Pre-proof

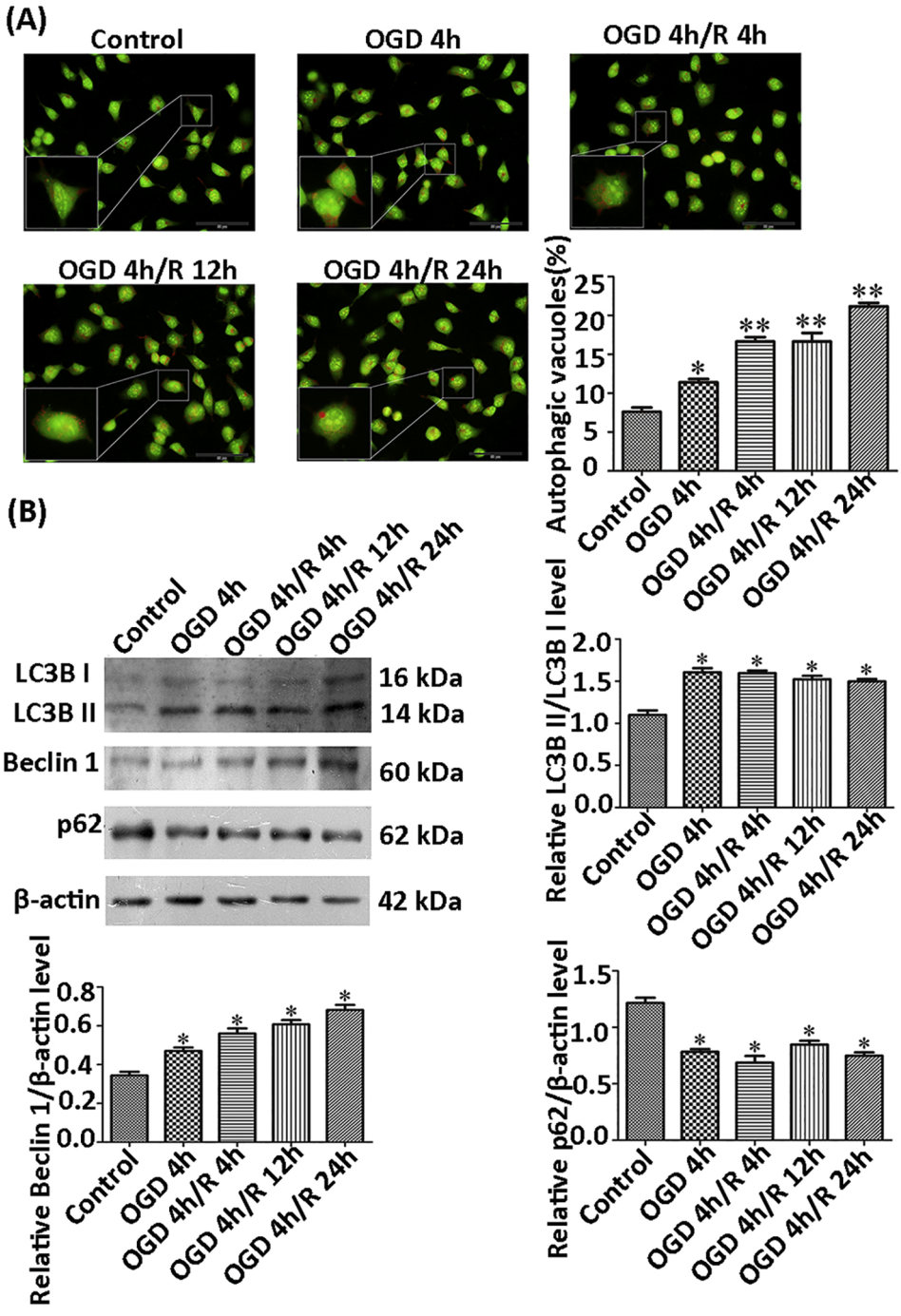
(A)
Control
OGD 4h
OGD 4h/R 4h
OGD 4h/R 12h
OGD 4h/R 24h
Autophagic vacuoles(%)
0
5
10
15
20
25
Control
OGD 4h
OGD 4h/R 4h
OGD 4h/R 12h
OGD 4h/R 24h
(B)
LC3B I
LC3B II
16 kDa
14 kDa
Beclin 1
60 kDa
p62
62 kDa
β-actin
42 kDa
Relative LC3B II/LC3B I level
0.0
0.5
1.0
1.5
2.0
Relative Beclin 1/β-actin level
0.0
0.2
0.4
0.6
0.8
Relative p62/β-actin level
0.0
0.5
1.0
1.5

Figure 1

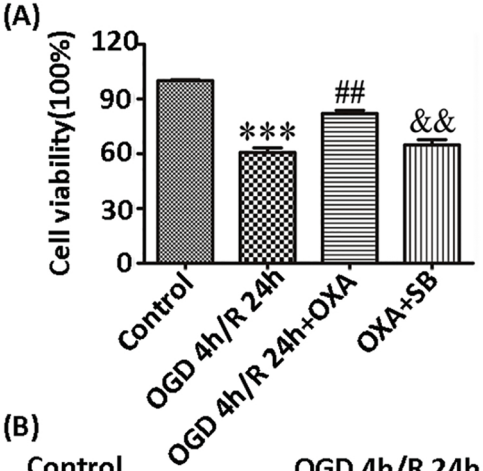
(A)
Cell viability(100%)
120
90
60
30
0
***
##
&&
Control
OGD 4h/R 24h
OGD 4h/R 24h+OXA
OXA+SB

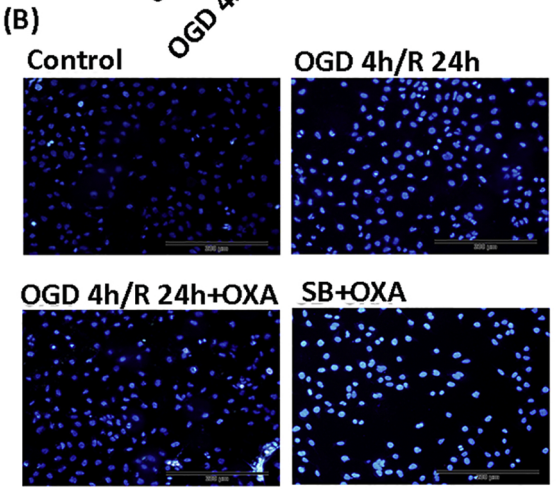
(B)
Control
OGD 4h/R 24h
OGD 4h/R 24h+OXA
SB+OXA

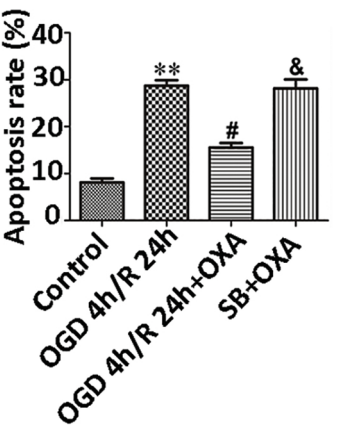
Apoptosis rate (%)
40
30
20
10
0
**
#
&
Control
OGD 4h/R 24h
OGD 4h/R 24h+OXA
SB+OXA

Figure 2

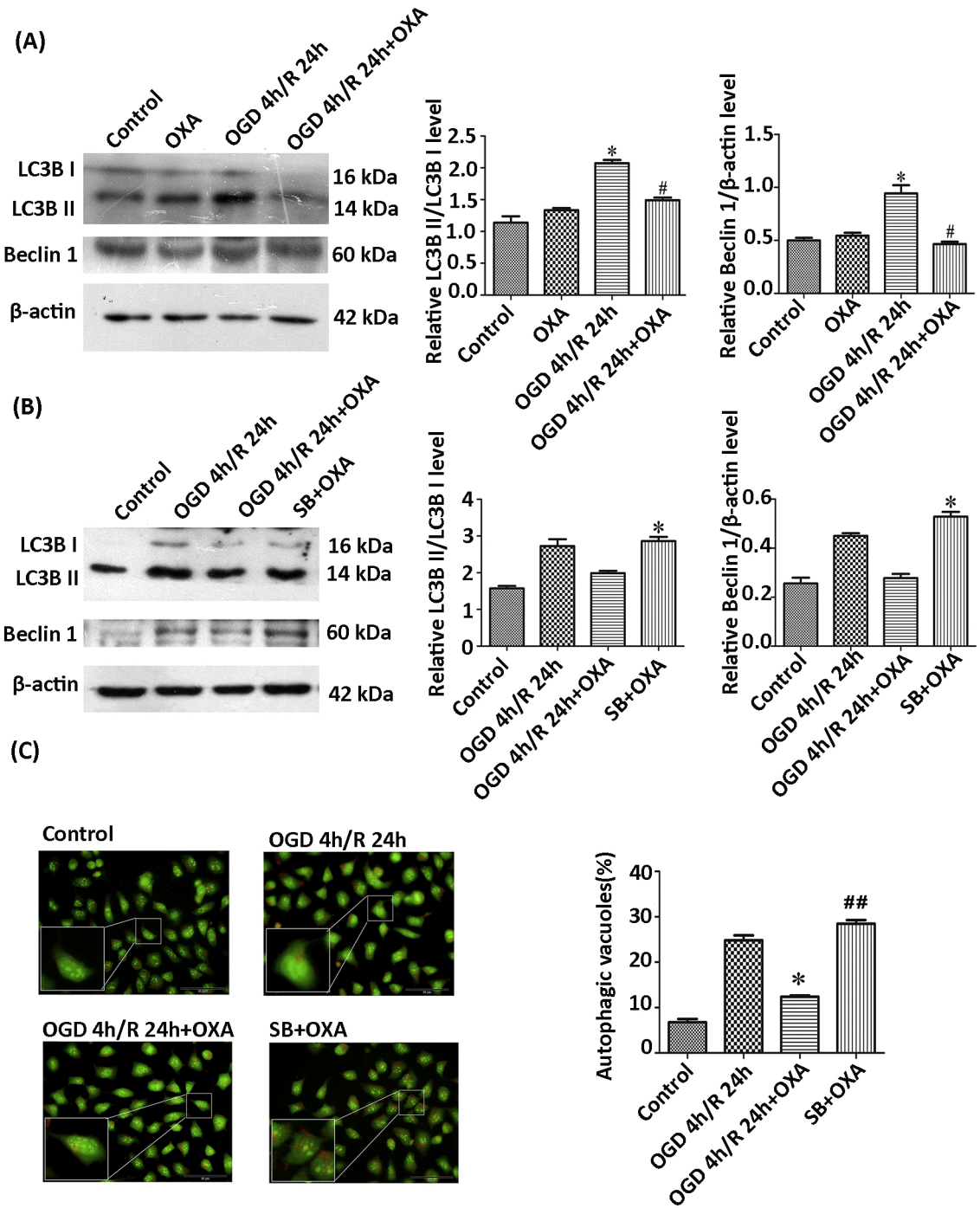
(A)
Control
OXA
OGD 4h/R 24h
OGD 4h/R 24h+OXA
LC3B I
LC3B II
16 kDa
14 kDa
Beclin 1
60 kDa
β-actin
42 kDa
Relative LC3B II/LC3B I level
Relative Beclin 1/β-actin level
(B)
Control
OGD 4h/R 24h
OGD 4h/R 24h+OXA
SB+OXA
LC3B I
LC3B II
16 kDa
14 kDa
Beclin 1
60 kDa
β-actin
42 kDa
Relative LC3B II/LC3B I level
Relative Beclin 1/β-actin level
(C)
Control
OGD 4h/R 24h
OGD 4h/R 24h+OXA
SB+OXA
Autophagic vacuoles(%)

Figure 3

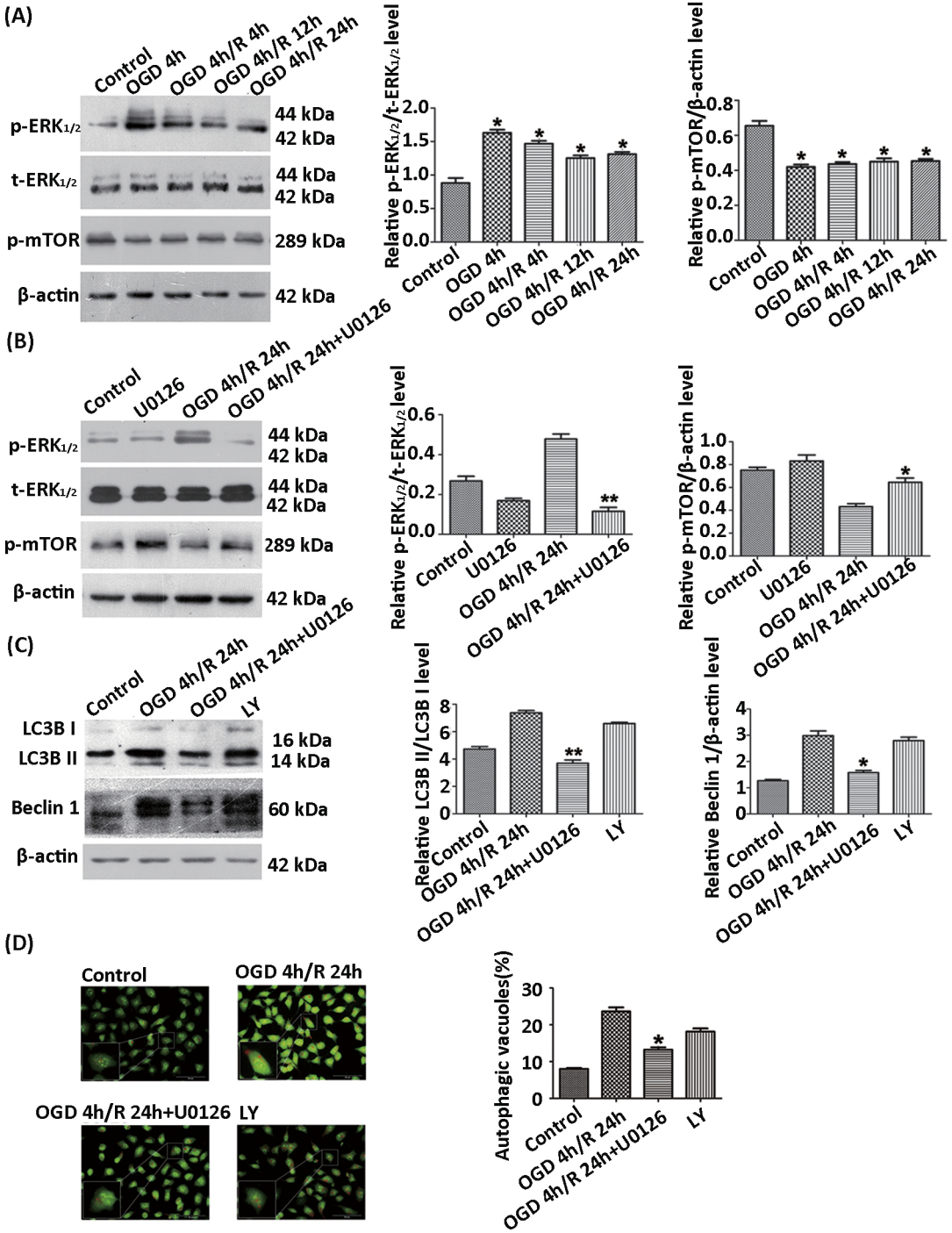
(A)
Control
OGD 4h
OGD 4h/R 4h
OGD 4h/R 12h
OGD 4h/R 24h
p-ERK1/2
t-ERK1/2
p-mTOR
β-actin
44 kDa
42 kDa
289 kDa
Relative p-ERK1/2/t-ERK1/2 level
Relative p-mTOR/β-actin level
(B)
U0126
OGD 4h/R 24h+U0126
Relative p-ERK1/2/t-ERK1/2 level
Relative p-mTOR/β-actin level
(C)
LY
LC3B I
LC3B II
Beclin 1
16 kDa
14 kDa
60 kDa
Relative LC3B II/LC3B I level
Relative Beclin 1/β-actin level
(D)
Autophagic vacuoles(%)

Figure 4

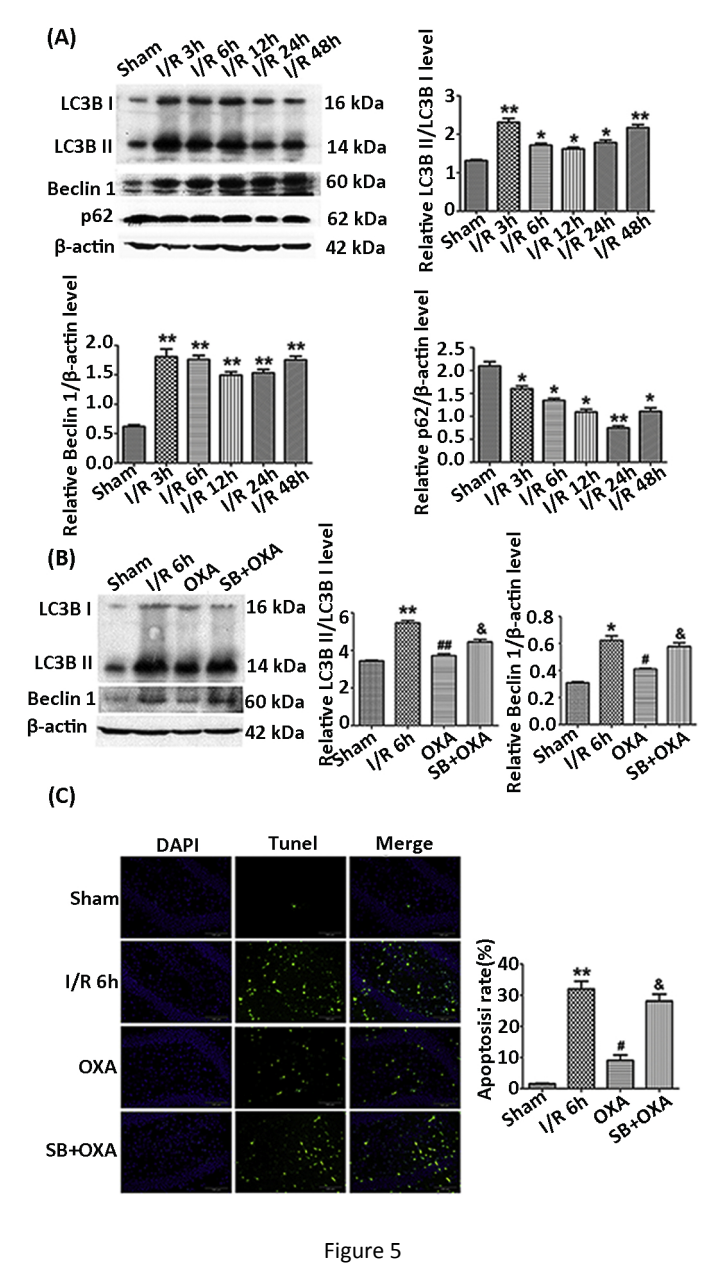
(A)
Sham
I/R 3h
I/R 6h
I/R 12h
I/R 24h
I/R 48h
LC3B I
LC3B II
Beclin 1
p62
β-actin
16 kDa
14 kDa
60 kDa
62 kDa
42 kDa
Relative LC3B II/LC3B I level
Relative Beclin 1/β-actin level
Relative p62/β-actin level
(B)
Sham
I/R 6h
OXA
SB+OXA
Relative LC3B II/LC3B I level
Relative Beclin 1/β-actin level
(C)
DAPI
Tunel
Merge
Sham
I/R 6h
OXA
SB+OXA
Apoptosisi rate(%)

Figure 5

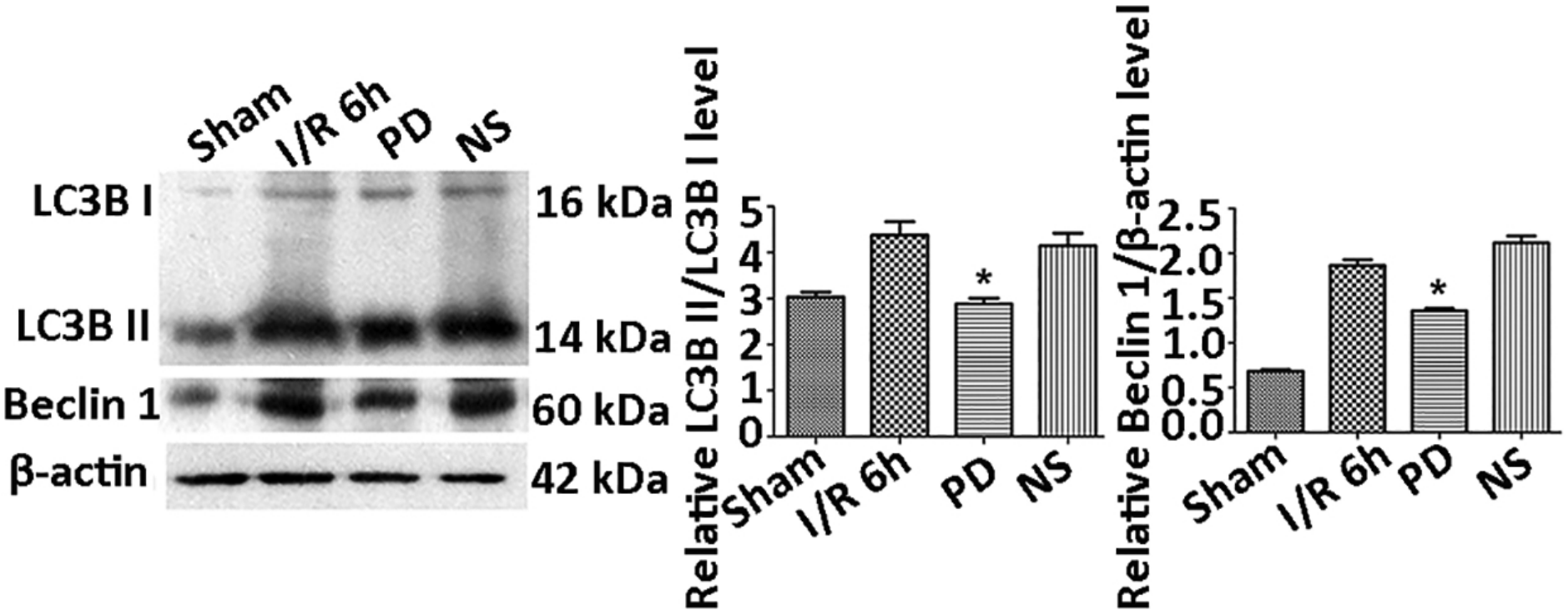
Sham
I/R 6h
PD
NS
LC3B I
LC3B II
Beclin 1
β-actin
16 kDa
14 kDa
60 kDa
42 kDa
Relative LC3B II/LC3B I level
0
1
2
3
4
5
*
Sham
I/R 6h
PD
NS
Relative Beclin 1/β-actin level
0.0
0.5
1.0
1.5
2.0
2.5
*
Sham
I/R 6h
PD
NS

Figure 6

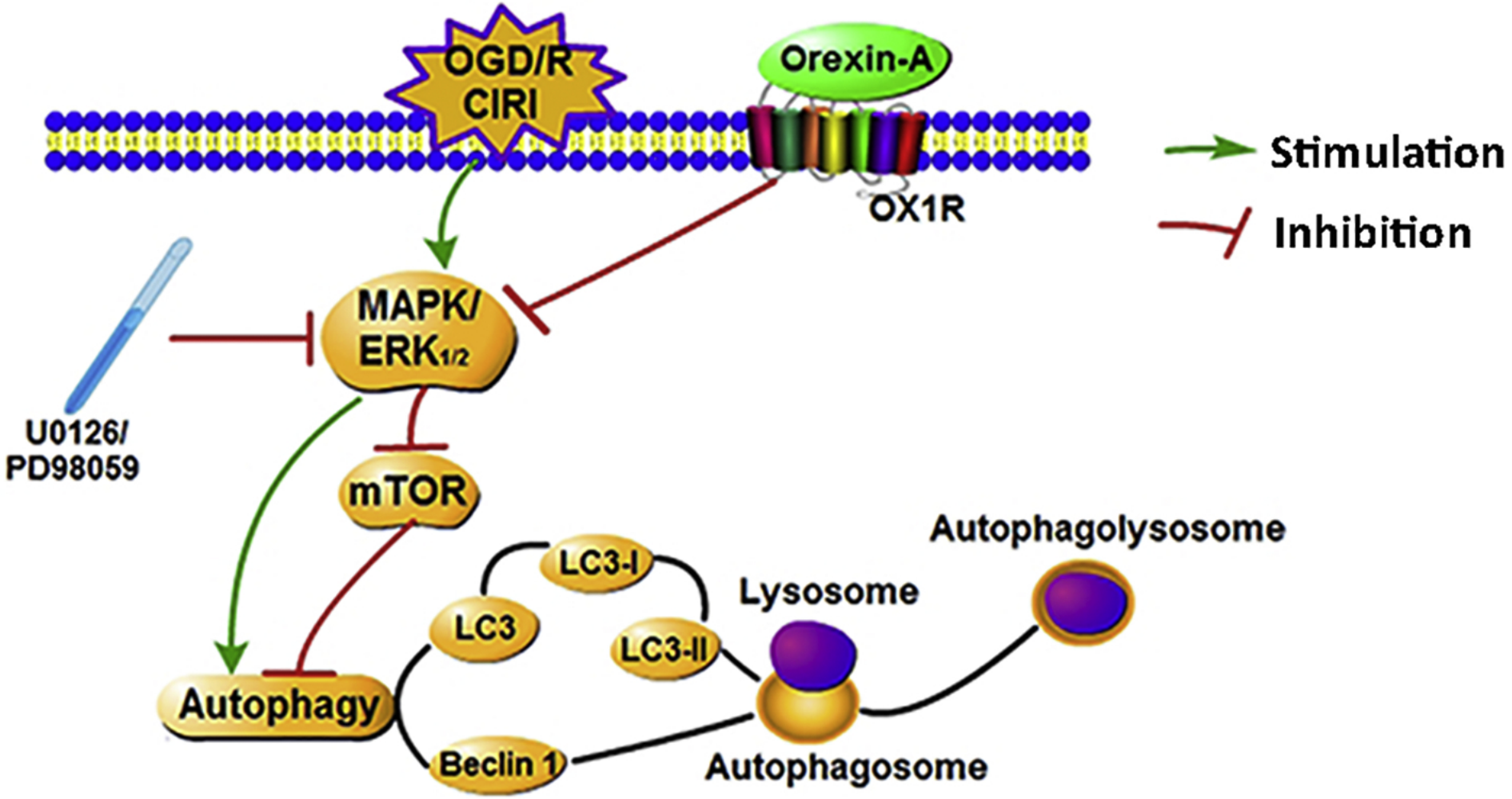
OGD/R
CIRI
Orexin-A
OX1R
Stimulation
Inhibition
MAPK/
ERK1/2
U0126/
PD98059
mTOR
LC3-I
LC3
LC3-II
Lysosome
Autophagolysosome
Autophagy
Beclin 1
Autophagosome

Figure 7